The Astrophysical Journal Letters, 887:L15 (4pp), 2019 December 10 https://doi.org/10.3847/2041-8213/ab59e0

Catastrophic Events in Protoplanetary Disks and Their Observational Manifestations

Tatiana V. Demidova[1] and Vladimir P. Grinin[2,3]
[1] Crimean Astrophysical Observatory, Nauchny, Crimea, Russia; proxima1@list.ru
[2] Pulkovo Observatory of the Russian Academy of Sciences, Pulkovskoje Avenue 65, St. Petersburg, Russia
[3] V.V. Sobolev Astronomical Institute, St. Petersburg University, Petrodvorets, St. Petersburg, Russia
Received 2019 August 26; revised 2019 November 18; accepted 2019 November 21; published 2019 December 10

Abstract

Observations of protoplanetary disks with high angular resolution using an ALMA interferometer showed that ring-shaped structures are often visible in their images, indicating strong disturbances in the disks. The mechanisms of their formation are vividly discussed in the literature. This article shows that the formation of such structures can be the result of destructive collisions of large bodies (planetesimals and planetary embryos) accompanied by the formation of a large number of dust particles, and the subsequent evolution of a cloud of dust formed in this way.

Unified Astronomy Thesaurus concepts: Protoplanetary disks (1300); Planetary system formation (1257); Hydrodynamical simulations (767)

1. Introduction

One of the most interesting results obtained using ALMA and VLT is the detection of substructures on images of protoplanetary disks observed with high angular resolution (see, e.g., van Boekel et al. 2017; Avenhaus et al. 2018; Benisty et al. 2018; Cazzoletti et al. 2018; Huang et al. 2018; Pérez et al. 2018). Statistical analysis shows (Huang et al. 2018) that the observed substructures often have a ring-like form, less often they look like wrapped spiral arms and very rarely exhibit crescent-like azimuthal asymmetries. The rings usually have fuzzy (blurred) boundaries. The origin of such structures is most often associated with disturbances that arise when planets interact with a protoplanetary disk (e.g., Ruge et al. 2013; Dong et al. 2015, 2017, 2018; van der Marel et al. 2015; Demidova & Shevchenko 2016; Jin et al. 2016; Bae et al. 2017). However, since no direct observational signs of the existence of planets in these disks were found, alternative models have also been considered (e.g., Banzatti et al. 2015; Birnstiel et al. 2015; Zhang et al. 2015; Okuzumi et al. 2016). Most of these models associate the formation of substructures with the development of various kinds of instabilities in disks (e.g., Johansen et al. 2009; Bai & Stone 2014; Takahashi & Inutsuka 2014; Dullemond & Penzlin 2018).

Below we show that the formation of observable structures can be the result of a collision of large bodies occurring in the disks during the formation of planetary systems. Such collisions play an important role in enlarging the embryos of the planets, from which planets are then formed (Chambers & Wetherill 1998; Kenyon & Bromley 2006, 2016). But not all collisions lead to the union of colliding bodies. In cases where the velocity of their relative motion is large enough, the collision process ends with the destruction of bodies. As a result, many smaller bodies and particles are formed. Such processes are cascade in nature, and they are described in the literature (see, e.g., Jackson & Wyatt 2012; Genda et al. 2015b). There is a lot of evidence that they occurred during the birth of the solar system. In particular, the widespread hypotheses about the origin of the Moon connects its formation with the destructive collision of the proto-Earth with a large body (Cameron & Ward 1976). The formation of the Mercury and origin of the Pluto–Charon system is associated with large impacts (Canup 2005; Stern et al. 2006; Benz et al. 2007; Canup 2011). It was suggested that the large obliquity of Uranus is also connected with the giant impact (e.g., Slattery et al. 1992).

It is obvious that the collisions of such large bodies, which result in the formation of a dust cloud, should be accompanied by flashes in the infrared region of the spectrum. In this connection, the results of Meng et al. (2014) are of great interest. They observed strong changes in the IR luminosity of a young star and interpreted them as the result of collisions of large bodies in a circumstellar disk (Meng et al. 2015; Su et al. 2019).

Jackson et al. (2014) showed that the asymmetries seen at large separations in some debris disks, like Beta Pictoris, could be the result of violent impacts. They also showed that after the impact the debris forms an expanding cloud that follows the progenitor object. The rate of the cloud shears depends on the velocity dispersion of the debris. But the dispersion of the cloud will typically take no more than one orbit. Then the initial debris clump is sheared out into a spiral structure. The shearing process will continue until the spiral has completely twisted into a ring during several orbits. The ring structure may be saved for 10^4 convolutions. The authors also showed that millimeter-size and larger grains will follow these distributions, while smaller grains will be blown-out by the radiation. We consider a similar model of disintegration of the dust cloud, but in the presence of gas.

2. Initial Condition

We assumed a model that consists of a young star of solar mass ($M_* = M_\odot$) embedded in a gas disk with total mass $M_{\rm disk} = 0.01 M_\odot$. At the beginning of simulation the disk matter was distributed to be azimuthally symmetrical within the radii $r_{\rm in} = 0.2$ and $r_{\rm out} = 100$ au. The initial density distribution of the disk is

$$\rho(r, z) = \frac{\Sigma_0}{\sqrt{2\pi} H(r)} \left(\frac{r}{r_{\rm in}}\right)^{-1.5} e^{-\frac{z^2}{2H^2(r)}}, \quad (1)$$

where Σ_0 is arbitrary scale parameter, which is determined by disk mass. Hydrostatic scale height is $H(r) = \sqrt{\frac{\kappa T_{\rm mid}(r) r^3}{G M_* \mu m_H}}$, where κ, G, and m_H are the Boltzmann constant, the gravitational constant, and the mass of a hydrogen atom. $\mu = 2.35$ is the mean molecular weight (Dutrey et al. 1994). Following

Chiang & Goldreich (1997) we determine the law of midplane temperature distribution $T_{\rm mid}(r) = \sqrt[4]{\frac{\phi}{4}}\sqrt{\frac{R_*}{r}}T_*$, where $\phi = 0.05$ (Dullemond & Dominik 2004). It was assumed that the disk is isothermal in the vertical direction along z. The temperature of the star was assumed to be $T_* = 5780$ K and the star radius was $R_* = R_\odot$.

A dust cloud (the result of collision) was placed at a distance of 30 au from the star. Its mass was 0.02% (approximately equal to half of the Moon mass) of the mass of the disk's dust component. It was supposed that the dust-to-gas mass ratio was 1/100 ($M_{\rm dust} = 10^{-4}M_\odot$). We simulate the cloud matter consisting of a number of particle types with different sizes from 1 μm to 1 mm with the density of dust particles equal to $\rho_d = 1$ g cm^{-3}. The particles of the cloud were distributed according to the law $\rho_w(x) \propto e^{-x}$, where x is the dimensionless distance from the center of the cloud, and the characteristic size of the cloud was $0.3H(r = 30) \approx 0.48$ au.

It was assumed that the dust cloud expands slowly during the process of orbital motion. So at the time $t = 0$ the velocity of motion of particles in the cloud is equal to the local Keplerian velocity at a given point of the disk plus random velocities of particles. The latter were distributed over a Gaussian with a mathematical expectation of $V = 50$ m s^{-1} and a standard deviation of 50 m s^{-1}.

3. Model Rationale

As stated in Section 1 the formation of the planetary system may be accompanied with catastrophic collisions of planet embryos or planetesimals. Su et al. (2019) showed that the formation of a small-dust cloud may take days to a month depending on the velocity of impact. The conclusions regarding the cascade destruction of colliding bodies were made for the models without gas; however, they are applicable to our model. At the periphery of the disk the gas density is low in order to significantly slow down the movement of debris. The density and temperature of the gas at 30 au are $\rho(30,0) = 7.5 \times 10^{-14}$ g cm^{-3} and $T(30) = 24$ K, the mean free path of a molecule is $\lambda = 2.4 \times 10^5$ cm, and the speed of sound is $c_s = 2.9 \times 10^4$ cm s^{-1}. Therefore the stopping time is $t_e = \frac{s\rho_d}{c_s\rho}$ for dust particles with size $s < \frac{9}{4}\lambda$ (Epstein regime in Weidenschilling 1977). For particles with $s = 1$ mm this time is 1.53 yr and it increases with s. Even this value is significantly more than the destruction time obtained in Su et al. (2019).

The critical energy (at which the target body loses at least half of its mass) was estimated assuming dependence on the radius of the body (e.g., Genda et al. 2015a). This dependence was extended to the case of planetary embryos by Marcus et al. (2009), which allowed us to estimate the critical velocity of a head-on collision of two bodies of quarter lunar mass $V_i \approx 5.42$ km s^{-1}. This value is approximately equal to the velocity of the Keplerian motion at a distance of 30 au ($V_k \approx 5.44$ km s^{-1}). But V_i increases with decreasing mass of the projectile body.

The initial mass of colliding planetesimals can be several times smaller than that accepted in our model. After the cascade process, the fragments' velocity of expansion should be larger than the two-body surface escape velocity ($v_{\rm esc}$). We assumed that the total mass of colliding planetesimals was equal to 10% ($m_d = 3.68 \times 10^{24}$ g) of that accepted in the model, and the initial cloud expansion velocity was $V_0 = 2.06v_{\rm esc} \approx 1.47$ km s^{-1} ($v_{\rm esc} \approx 0.72$ km s^{-1}). The velocity of dust particle size of 1 mm decreased according to the law $V(t) = V_0 e^{-t/te}$ due to the gas drag forces to a value $V = 50$ m s^{-1} during $T \approx 5.16$ yr. The cloud expanded and its size reached $\Delta r \approx 0.48$ au. Since planetesimals are present in the disk, we assume that 90% of dust matter is a large particle, which settled down to the disk plane. The fragments of the cloud exchange momentum with the disk particles, which in turn become a part of the cloud. Since the surface density of the dust at 30 au is $\Sigma_d(30) = 0.045$ g cm^2 the cloud particles can interact with dusty matter with mass $M_{dd} = 0.9\Sigma_d(30)\int_0^T\int_0^{\Delta r}\frac{V_k dt}{2r}[(r+dr)^2 - (r-dr)^2]dr = 0.9\Sigma_d(30)2V_kV_0\int_0^T[\int_0^t e^{-t'/te}dt']dt \approx 3.31 \times 10^{25}$ g orbiting over time T. The sum of the masses $M_{dd} + m_d = 3.68 \times 10^{25}$ g is equal to the mass accepted in our model. In that case the critical velocity of impact is $V_i \approx 2.52$ km s^{-1}. However, the probability of collision of such planetesimals in the absence of external influence is negligible. Therefore, a mechanism is needed to disperse the planetary embryo to high speed.

We suppose that a giant planet may be responsible for the scattering of solid bodies to the outer part of the disk at high speeds. The eccentricity and inclination of particle orbits will be damping due to resonant interactions with a gas disk on the secular timescale (see, e.g., Kley & Nelson 2012). But the orbit of planetary embryos may cross the planetary chaotic zone during the migration of one or several planets. Batygin & Morbidelli (2013) showed that the semimajor axis and eccentricity of the particles may change significantly on an orbital timescale under the condition of rapid dynamical chaos. This mechanism can contribute to the transfer of planetary embryos to the periphery of the disk. Some of them leave their initial position at high velocity (Morrison & Malhotra 2015). Kenyon & Bromley (2008) showed that the process of planetary embryo formation in the outer part of the protoplanetary disk proceeds more slowly than in the inner one. However, several hundred ~100 km planetesimals can exist on the periphery of the disk and may collide with scattering planetary embryos.

4. Simulation

We calculated the evolution of the cloud in gas surroundings using the smooth particle hydrodynamics method. The calculations of the dust particle dynamics in the gaseous medium were performed using the code Gadget-2 (Springel et al. 2001; Springel 2005) modified in Demidova (2016). Equations describing the interaction of dust and gas from Laibe & Price (2014) were added to the code. In total, 2×10^5 particles with gas properties and 5×10^4 with dust properties took part in the simulation.

The dust opacity is calculated using Mie theory for magnesium–iron silicates (Dorschner et al. 1995). The RADMC-3D code was used for the 3D radiative transfer calculations, which is an open code available online at http://www.ita.uni-heidelberg.de/~dullemond/software/radmc-3d/.

5. Results and Discussion

The results of the hydrodynamic calculations are presented on Figure 1. We see that, due to the differential rotation of the Keplerian disk, the dust cloud stretches and successively takes all three forms described above: a piece of arc resembling a cyclonic vortex and a tightly wound spiral, which then turns into a ring.

To calculate the observable images of the disk it was assumed that 10% of dust mass is in small grains (0.1 μm), which determine

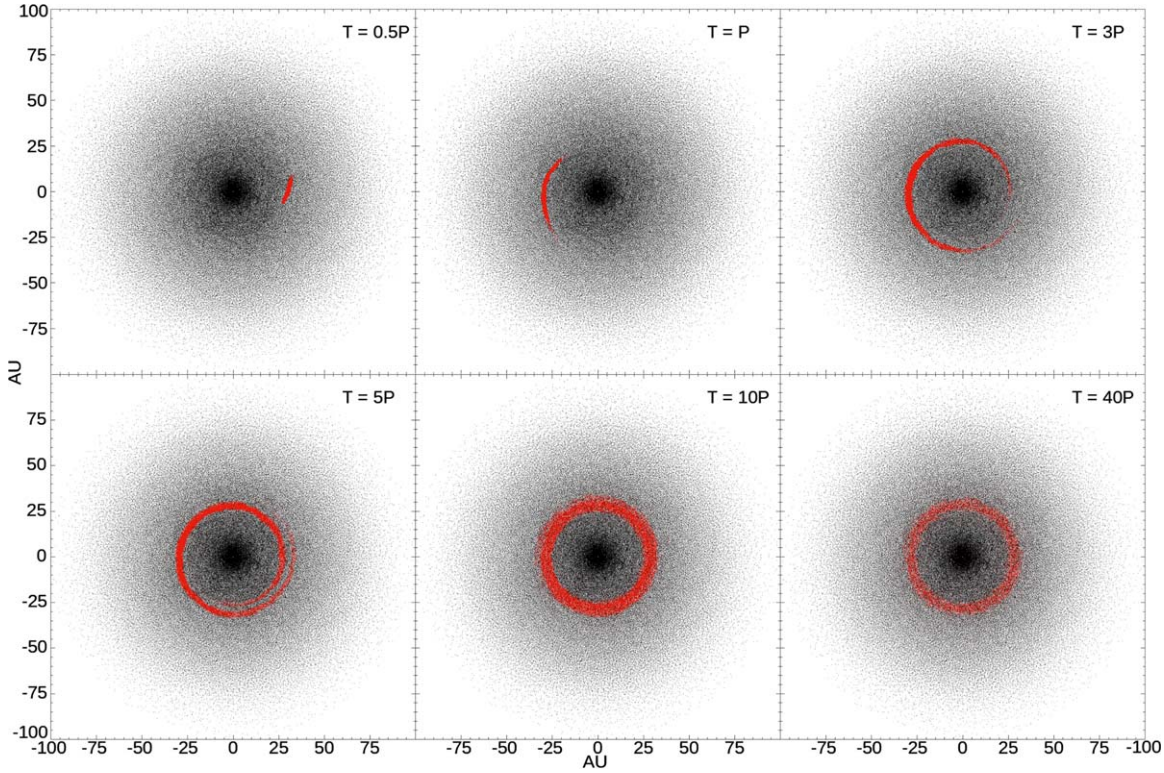

Figure 1. Particle distribution in the model. Gas particles are shown in black and dust particles are red dots. The time in the upper left corner of the images is indicated in the orbital periods of the cloud center (P).

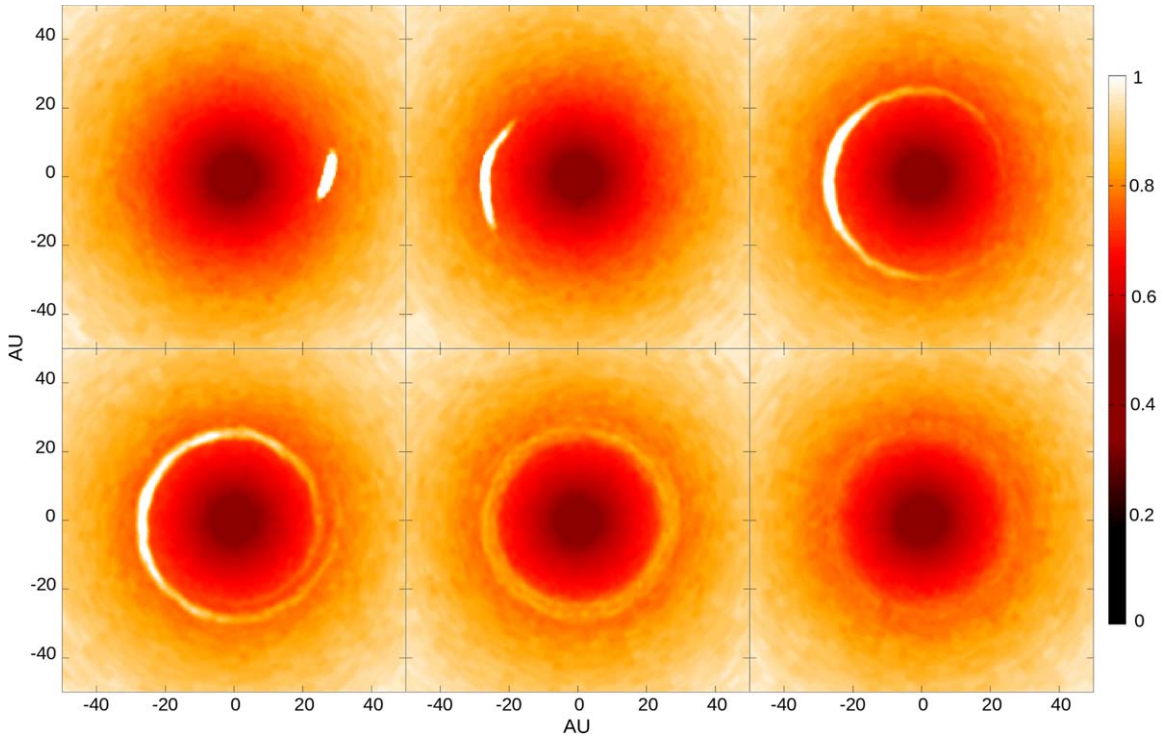

Figure 2. Disk images at wavelength 1.3 mm. The color shows the intensity of radiation multiplied by R^2 in arbitrary units. The time points are in accordance with Figure 1.

the disk temperature structure, and such particles are well mixed with the gas matter. The images of the disk on the wavelength 1.3 mm are presented on Figure 2. Naturally the particles of 1 mm give the greatest contribution to the luminosity of the structure. Whereas particles of 10 μm and less are quickly dispersed by gas and can be considered well mixed with gas.

The contrast of the structures formed by cloud matter is determined by the contribution of small dust to the background

thermal radiation of the disk. The structures at the initial stages of cloud disintegration are also visible when 100% of the matter of the disk's dust is small dust. However, at later stages, the contrast of the structure decreases considerably.

According to Figure 1 the transition from a crescent-like structure to a ring occurs during several revolutions. The ring exists much longer, during several dozen revolutions. Its borders are gradually diffused with time. Calculations have shown that the speed of transition from the cloud to the ring depends on the velocity of dust cloud expansion. The process may last a dozen revolutions in the model with zero expanding velocity. Immediately after the collisions the embryos' fragment velocities will be high (comparable to the collision speeds). They are diminished in cascade collisions and by the interaction with the protoplanetary disk. As a result, the fragments become smaller and slow down their movement to the exchange of momentum with the surrounding matter, which becomes a part of the primary cloud. This means that the initial mass of colliding bodies may be significantly less than that adopted in our model, and accordingly, the collision velocity should be much smaller.

The advantage of our model is that it is based on a physical process (catastrophic collisions of the massive bodies) for which observational manifestations have evidential facts in the history of the solar system. Such destructive collisions can probably be initiated by one or several giant planets in the process of their migration. As mentioned in Section 1 a giant planet can form a ring-shaped structure in a protoplanetary disk, and a giant impact could produce another one. Thus, the considered model contributes to the explanation of the multiple rings in the protoplanetary disk images.

We assume that the formation of giant planets may be accompanied by several destructive collisions of planetary embryos. To confirm this hypothesis, numerical calculations on secular timescales are required, as well as taking the gas presence into account. If it is confirmed by further research, this will allow for the observation of the consequences of catastrophic collisions at the birth of other planetary systems by methods of interferometry.

It is a pleasure to thank the referee for valuable and useful remarks. T.V.D. is supported by the Russian Science Foundation under grant 19-72-10063. V.P.G. is supported by the Program of Fundamental Research of the Russian Academy of Sciences under grant KP19-270.

ORCID iDs

Tatiana V. Demidova https://orcid.org/0000-0001-7035-7062

References

Avenhaus, H., Quanz, S. P., Garufi, A., et al. 2018, ApJ, 863, 44
Bae, J., Zhu, Z., & Hartmann, L. 2017, ApJ, 850, 201
Bai, X.-N., & Stone, J. M. 2014, ApJ, 796, 31
Banzatti, A., Pinilla, P., Ricci, L., et al. 2015, ApJL, 815, L15
Batygin, K., & Morbidelli, A. 2013, A&A, 556, A28
Benisty, M., Juhász, A., Facchini, S., et al. 2018, A&A, 619, A171
Benz, W., Anic, A., Horner, J., & Whitby, J. A. 2007, SSRv, 132, 189
Birnstiel, T., Andrews, S. M., Pinilla, P., & Kama, M. 2015, ApJL, 813, L14
Cameron, A. G. W., & Ward, W. R. 1976, LPSC, 7, 120
Canup, R. M. 2005, Sci, 307, 546
Canup, R. M. 2011, AJ, 141, 35
Cazzoletti, P., van Dishoeck, E. F., Pinilla, P., et al. 2018, A&A, 619, A161
Chambers, J. E., & Wetherill, G. W. 1998, Icar, 136, 304
Chiang, E. I., & Goldreich, P. 1997, ApJ, 490, 368
Demidova, T. V. 2016, Ap, 59, 449
Demidova, T. V., & Shevchenko, I. I. 2016, MNRAS, 463, L22
Dong, R., Li, S., Chiang, E., & Li, H. 2017, ApJ, 843, 127
Dong, R., Li, S., Chiang, E., & Li, H. 2018, ApJ, 866, 110
Dong, R., Zhu, Z., & Whitney, B. 2015, ApJ, 809, 93
Dorschner, J., Begemann, B., Henning, T., Jaeger, C., & Mutschke, H. 1995, A&A, 300, 503
Dullemond, C. P., & Dominik, C. 2004, A&A, 421, 1075
Dullemond, C. P., & Penzlin, A. B. T. 2018, A&A, 609, A50
Dutrey, A., Guilloteau, S., & Simon, M. 1994, A&A, 286, 149
Genda, H., Fujita, T., Kobayashi, H., Tanaka, H., & Abe, Y. 2015a, Icar, 262, 58
Genda, H., Kobayashi, H., & Kokubo, E. 2015b, ApJ, 810, 136
Huang, J., Andrews, S. M., Pérez, L. M., et al. 2018, ApJL, 869, L43
Jackson, A. P., & Wyatt, M. C. 2012, MNRAS, 425, 657
Jackson, A. P., Wyatt, M. C., Bonsor, A., & Veras, D. 2014, MNRAS, 440, 3757
Jin, S., Li, S., Isella, A., Li, H., & Ji, J. 2016, ApJ, 818, 76
Johansen, A., Youdin, A., & Klahr, H. 2009, ApJ, 697, 1269
Kenyon, S. J., & Bromley, B. C. 2006, AJ, 131, 1837
Kenyon, S. J., & Bromley, B. C. 2008, ApJS, 179, 451
Kenyon, S. J., & Bromley, B. C. 2016, ApJ, 825, 33
Kley, W., & Nelson, R. P. 2012, ARA&A, 50, 211
Laibe, G., & Price, D. J. 2014, MNRAS, 440, 2147
Marcus, R. A., Stewart, S. T., Sasselov, D., & Hernquist, L. 2009, ApJL, 700, L118
Meng, H. Y. A., Su, K. Y. L., Rieke, G. H., et al. 2014, Sci, 345, 1032
Meng, H. Y. A., Su, K. Y. L., Rieke, G. H., et al. 2015, ApJ, 805, 77
Morrison, S., & Malhotra, R. 2015, ApJ, 799, 41
Okuzumi, S., Momose, M., Sirono, S.-i., Kobayashi, H., & Tanaka, H. 2016, ApJ, 821, 82
Pérez, L. M., Benisty, M., Andrews, S. M., et al. 2018, ApJL, 869, L50
Ruge, J. P., Wolf, S., Uribe, A. L., & Klahr, H. H. 2013, A&A, 549, A97
Slattery, W. L., Benz, W., & Cameron, A. G. W. 1992, Icar, 99, 167
Springel, V. 2005, MNRAS, 364, 1105
Springel, V., Yoshida, N., & White, S. D. M. 2001, NewA, 6, 79
Stern, S. A., Weaver, H. A., Steffl, A. J., et al. 2006, Natur, 439, 946
Su, K. Y. L., Jackson, A. P., Gáspár, A., et al. 2019, AJ, 157, 202
Takahashi, S. Z., & Inutsuka, S.-i. 2014, ApJ, 794, 55
van Boekel, R., Henning, T., Menu, J., et al. 2017, ApJ, 837, 132
van der Marel, N., van Dishoeck, E. F., Bruderer, S., Pérez, L., & Isella, A. 2015, A&A, 579, A106
Weidenschilling, S. J. 1977, MNRAS, 180, 57
Zhang, K., Blake, G. A., & Bergin, E. A. 2015, ApJL, 806, L7